

SECONDARY DROPLET ATOMISATION FROM SINGLE DROP IMPACT ON HEATED SURFACES

G.E. Cossali, M. Marengo, M. Santini and J. Watanabe

Corresponding author: cossali@unibg.it

*Università di Bergamo-Facoltà di Ingegneria- 24044 Dalmine (BG) - Italy

Abstract

The paper reports an experimental analysis of impact of single drops on a solid heated surface at different temperatures, so as to consider different heat exchange regimes from nucleate boiling to film boiling. Secondary drops produced after impact were characterised by measuring size and velocity both using PDA and the analysis of high resolution images (IAT). Two impacting walls with different surface roughness were used to show the effect of this parameter on different atomisation regimes. Image analysis allowed also to define the details of the morphology of drop spreading and break-up.

Introduction

The study of drop impact onto solid heated surfaces is important in many industrial applications, such as the metal surface cooling in the steel industry and in the nuclear power plants, the hot coating of surfaces, the diesel and gasoline direct injection, the thermal control of electronic devices. When the surface is not heated, three main phenomenological outcomes are expected: the drop deposition on the solid surface, a complex process through which secondary droplets are generated (secondary atomisation), and either a complete or a partial drop rebound from the surface (see also [1]). For a heated surface, the impact process has different characteristics. The boiling start-up during the drop spreading radically changes the impact dynamics. The secondary atomisation is generated not through the so called “crown splash” [2], but because of the vapour bubble explosion at the liquid interface of the spreading lamella. The impact velocity and the surface temperature, the impact angle, the surface tension and viscosity of the liquid, the surface wettability, effusivity and roughness are the main parameters influencing the process. The importance of the last three parameters can be inferred by the numerous works available in the open literature [3, 4, 5, 6, 7, 8]. As the time scale of heat transfer is large compared to the spreading time scale, the drop impact in the first phase may be considered adiabatic, hence the surface temperature is not a influencing parameter [9]. When the contact area between liquid and solid surface increases, the heat transfer becomes relevant and during the spreading starts a nucleate boiling process with the generation of bubbles and secondary droplets [10]. Varying the surface temperature, three regimes are evidenced: a) surface temperatures near to the liquid saturation temperature, b) surface temperatures below the Nukijama temperature, c) surface temperatures below the Leidenfrost temperature. In the second regime (b) the spreading process on surface has very unstable characteristics: after reaching a maximum diameter, even for low Weber numbers, there is a strong contraction of the lamella with production of secondary droplets [11]. For higher temperatures, the lamella may break-up in liquid ligaments without generating a crown; besides the liquid bulk on the surfaces tends to break-up and rebound [11]. Akao et al. [12] found different critical Weber numbers using different liquids and drop diameter. Xiong e Yuen [13] confirmed this observation showing that the dimensional scaling with the Weber number appears to be not valid for sub-millimetric droplets. For surface temperature above the Leidenfrost temperature, the formation of a vapor film during the liquid spreading lead to a rather different impact morphology, and Wachters e Westerling [14] were the first to describe quantitatively the secondary atomization regimes. Because the Leidenfrost temperature has a phenomenological definition it also depends on the dynamics parameters, such as the impact velocity and angle [15].

Experimental set-up

The impacting system comprises an aluminium alloy (AlMg3) circular disc, electrically heated from below and temperature larger than 330°C can be reached and maintained by PC-based PID controller through the feedback supplied by a thermocouple positioned under the centre of the impacting wall. The drop generator is made by needles (whose internal diameters may be changed from 0.16mm to 2 mm) connected through a flexible pipe to a small pressurised tank containing the working liquid. A simple system, based on a throttling of the flexible pipe, allows to vary the flow rate and then the drop frequency. Drop diameter may range between 1.9 to 4.7 mm. The drop impact velocity is obtained by gravitational acceleration and may range between 0 to about 6m/s. A CCD camera (SensiCam PCO, Colour, 1280x1024 pixels) is used to acquire the images of the impact. The CCD acquisition and illumination systems are driven by a light barrier system (comprising a small He-Ne laser and a

photodiode connected through an amplifier to the experiment governing system). To obtain enough luminosity with continuous back illumination, acquisition times from 5 to 20 μ s were used. A commercial image analysis code (Image ProPlus) was used as main environment to develop home built routines for measuring output parameters like average drop diameter, roundness, etc. A Dantec PDA (Phase Doppler Anemometer) was used to measure simultaneously the secondary drop velocity and size. The particular set-up was designed by means of a purpose built code to minimise the effect of lack of knowledge on refracting index as temperature of secondary droplets is not known. The set-up consented to measure drop size from 2 μ m to 250 μ m and this overlaps partially the range allowed by using the CCD camera (from 30 μ m to few mm), allowing to reconstruct the entire drop size PDF from 2 μ m to few mm. Only the vertical drop velocity was acquired. The measurements were triggered by the same system described above, allowing the acquisition of measurements for many different drop impacts, to obtain statistically significant samples.

Results and discussion

The main aim of the work was to show the characteristics (both qualitative and quantitative) of the secondary atomisation produced by the impact between a liquid drop and a hot surface. As the objective was to evidence the sole effect of heat transfer on secondary atomisation only one dynamic regime was investigated (using distilled water drop of 2.1mm diameter (D_0) and impacting velocity (V_0) of 3.13m/s) that would not produce secondary atomisation if the surface were not heated. Two very different surface roughness were analysed ($R_z=1.6\mu$ m and 14.5 μ m, where R_z is defined as the arithmetic mean of 5 single maximum heights $[Z]_i$ within 5 parts of length $0.2 l_m$ from the line of measurement (l_m) according to $R_z = 0.2(Z_1 + Z_2 + Z_3 + Z_4 + Z_5)$) to show possible effects of this parameter on secondary atomisation. Non-dimensional time defined as: $\tau=tV_0/D_0$ will be used in the following.

Morphology

Two main regimes of secondary atomisation are expected to exist as a function of wall temperature, which can be related to the two boiling regimes: i) *bubble boiling*, when bubbles, produced by the heat transfer between the wall (whose temperature is obviously larger than the liquid boiling temperature), grow and rupture producing a plethora of small secondary drops; ii) *film boiling*, when the wall temperature is sufficiently high to generate a

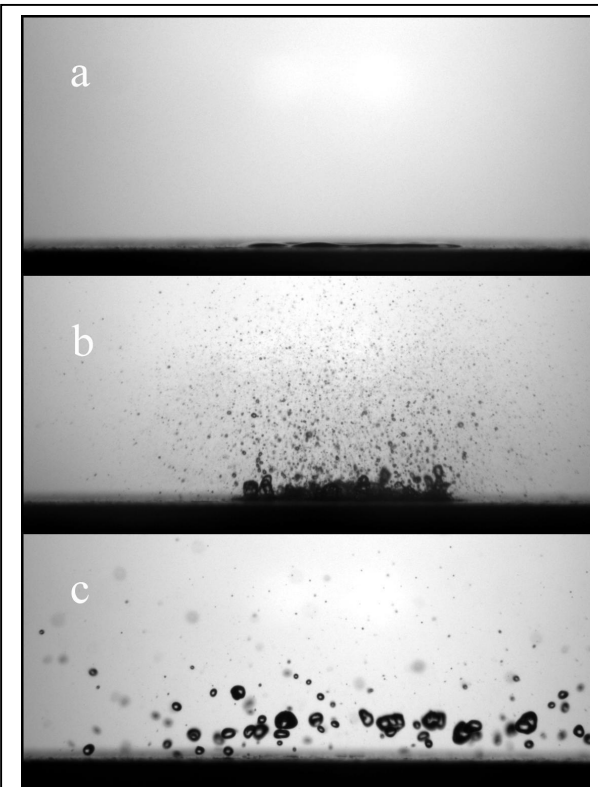


Figure 1. Comparison among results of impact at different wall temperature (a) $T_w=70^\circ\text{C}$, b) $T_w=150^\circ\text{C}$, c) $T_w=260^\circ\text{C}$) under the same impacting conditions ($D_0=2.1\text{mm}$, $V_0=3.13\text{m/s}$) at the same time $\tau=tV_0/D_0=11$)

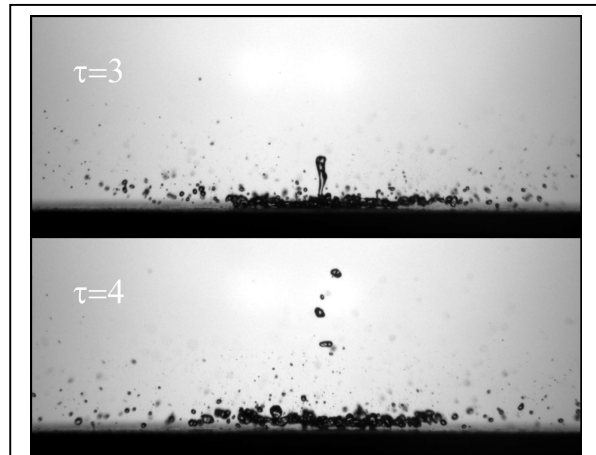


Figure 2. Central jet generation after the impact of a water drop ($D_0=2.1\text{mm}$, $V_0=3.13\text{m/s}$) for $T_w=260^\circ\text{C}$ at different times after impact ($\tau=3$ and $\tau=4$).

vapour film, almost immediately after impact, that may levitate the liquid from the wall. The image acquisition technique allowed to evidence those regimes and fig. 1 shows the comparison relative to the impacting conditions above mentioned at different wall temperatures. The comparison to the picture taken for $T_w=70^\circ\text{C}$ (below saturation temperature) shows how the secondary atomisation is due only to thermal (boiling) effects as inertia is not enough to produce secondary atomisation. It is interesting to observe the existence of a relatively large drop at the centre of the image for the case at 260°C (above

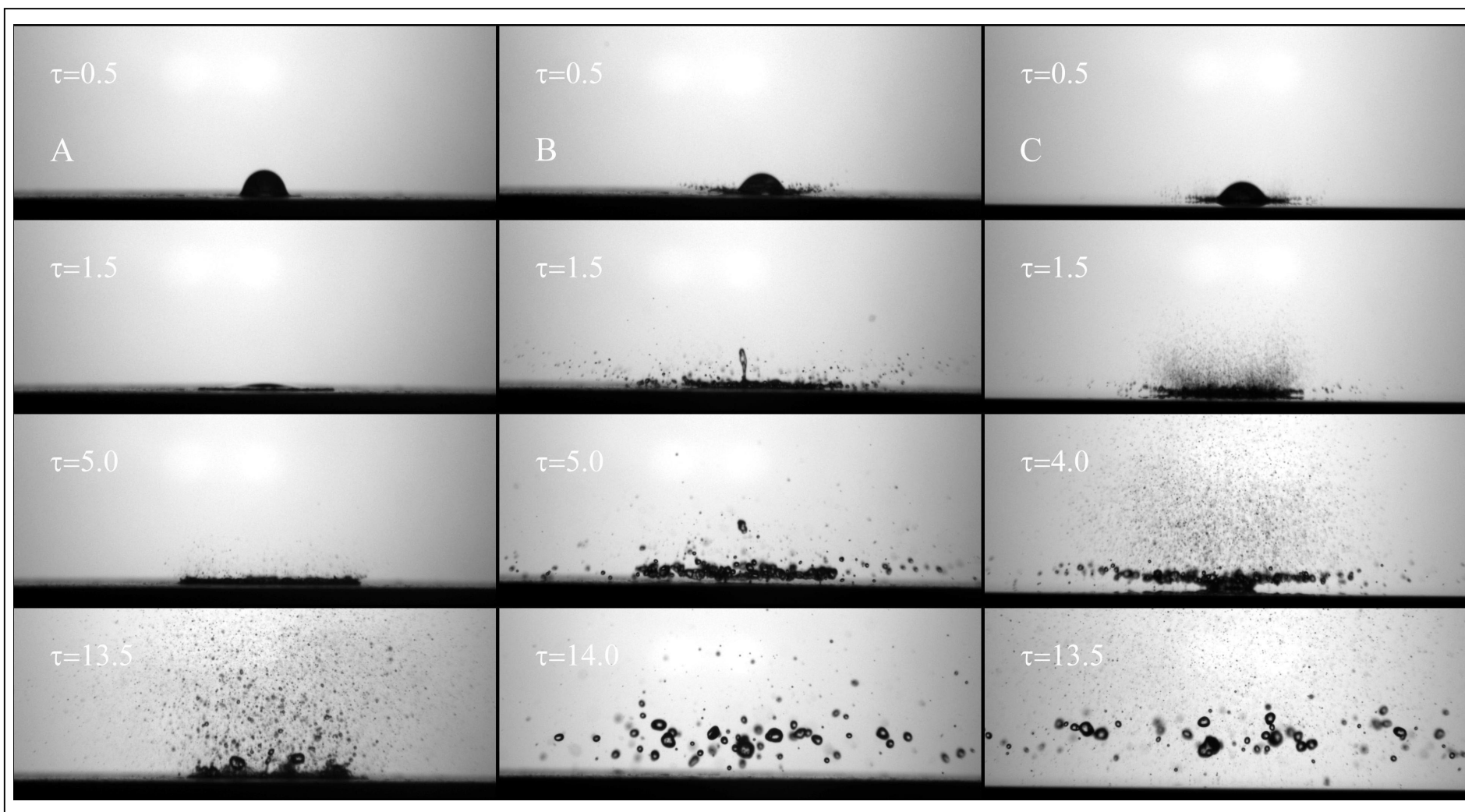


Figure 3. Comparison between bubble boiling on rough surface ($T=150^\circ\text{C}$, $R_z=14.5\mu\text{m}$, column a), film boiling on rough surface ($T=260^\circ\text{C}$, $R_z=14.5\mu\text{m}$, column b) and film boiling on smooth surface ($T=260^\circ\text{C}$, $R_z=1.6\mu\text{m}$, column c).

Leidenfrost temperature), which is produced by the break up of a sort of central Rayleigh jet (figures 2 show better the effect) which is produced just at the beginning of the spreading phenomenon ($\tau=3$ and $\tau=4$).

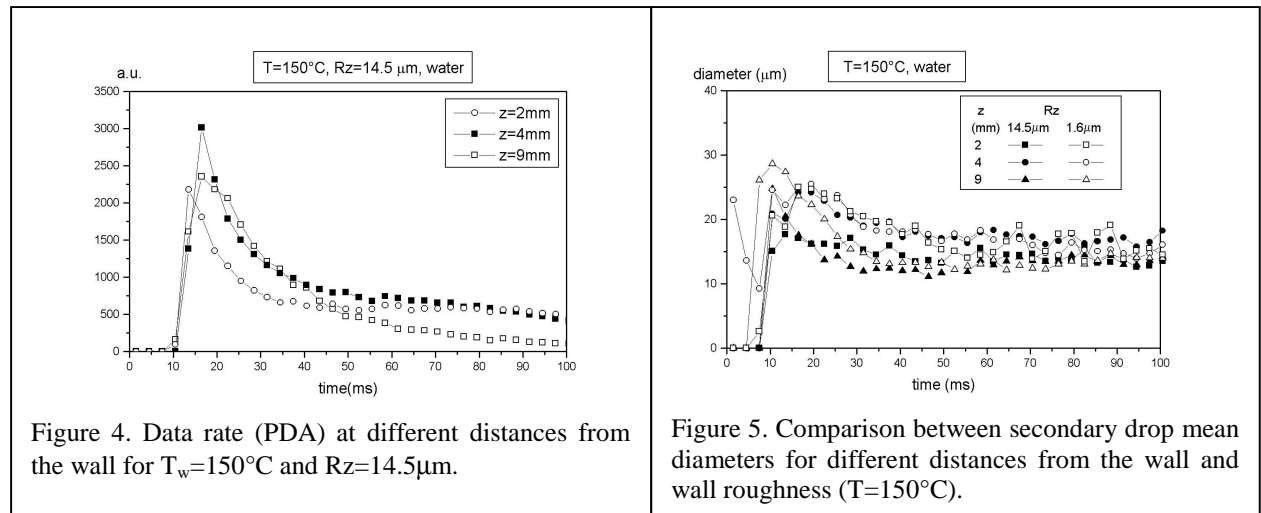
Another important difference between the two regimes is the characteristic times at which the secondary atomisation starts. In bubble boiling regime the formation of first secondary droplets, produced by the break-up of thin jets protruding from the film and due to the explosion of vapour bubbles (as shown by [16]), start few milliseconds after impact (see figure 3a) whereas the secondary drop production starts immediately after impact for film boiling regime (see figure 3b). Also the secondary drop direction is very different: mainly vertical for bubble boiling, ejection in radial direction for the film boiling (during the very first impacting period). Finally, for the film boiling regime, the presence of a vapour film produces the levitation of relatively large droplets coming from the break up of the film layer (figures 3b). To analyse the effect of surface roughness on the morphology of secondary atomisation, images were acquired at same times after impact for two different surface roughness ($1.6\mu\text{m}$ and $14.5\mu\text{m}$) for both boiling regimes. For the bubble boiling regime ($T=150^\circ\text{C}$) the difference is mainly on spreading that appears faster for larger roughness and atomisation appears to become effective earlier. For film boiling (figure 3b and 3c) the effect is quite evident: no central jet is observed for the smoother surface impact (figure 3c) and a larger secondary droplet production (quite similar to the bubble boiling droplet production) is observed in the early stage. A deeper investigation is clearly needed to discover the causes of those phenomena.

2. Secondary droplet size and velocity

From images similar to those presented in the above mentioned figures, the purpose built image analysis routines allowed to evaluate the size of the secondary droplets. The spatial accuracy allowed to measure only droplets larger than $30\mu\text{m}$. Moreover, the routines allowed to acquire not only the mean size of the droplets but also parameters like minimum and maximum diameter, size of the rectangle enclosing each droplets, etc. In this way the droplets having large eccentricity may be rejected in any post processing procedure used for evaluating mean size or other momenta. To enlarge the measured size range toward smaller sizes, the PDA was set up and the experiment repeated performing measurements at different locations above the impact point in a square region ($6\text{mm}\times 6\text{mm}$) at three different distances from the wall (2,4 and 9mm). The chosen PDA set-up allowed to measure drop size in the range $2\text{--}250\mu\text{m}$ together with vertical (normal to the wall) velocity component. The two observed atomisation regimes will be analysed below.

2.1. Bubble boiling regime ($T_w=150^\circ\text{C}$) and rough surface ($R_z=14.5\mu\text{m}$)

For the surface having larger roughness ($R_z=14.5\mu\text{m}$) the variation of size and velocity with x and y coordinates (in the analysed region) was found to be neglectful. The drop data rate (which is related to the mass flow rate through the measurement volume) depends strongly on time during the first 4ms after drop impact and also later there is a mild dependence (fig.4). The d_{10} evaluated for the size range between 2 and $250\mu\text{m}$ (the PDA measuring range) shows a slight dependence on time after drop impact (ADI): the initial period (about 30ms ADI) is characterised by an average size slightly larger than that found later (Fig 5)) independent of the distance from the wall, the average velocity instead (Fig. 6) shows an obvious dependence on wall distance, clearly due to the action of the drag (as gravity effects are neglectful on those distances) on the ejected droplets, and a decrease with time. No velocity size correlation appears to exist. The image analysis allowed to measure the drop diameter in the range $30\text{--}800\mu\text{m}$ and from those measurements the diameter PDF was evaluated. Then, in order to compare to the results obtained with PDA, a scaling of the two PDFs was performed by equating the values in the region where the two size ranges overlap obtaining a sort of “extended” PDF (see figure 7). The analysis confirm that, for this regime and wall roughness, the extended PDFs do not depend on the distance from the wall. It is of a certain interest to observe (see tab1) that although the mean diameter (d_{10}) evaluated on the PDA data is quite close to that evaluated on the extended distribution (discrepancy about 10%) the SMD (d_{32}), as expected, is strongly different as the bigger drops detected by IAT play an important role in increasing d_{32} .



2.2. Bubble boiling regime ($T_w=150^\circ\text{C}$) and smooth surface ($Rz=1.6\mu\text{m}$)

Also for the smooth surface ($Rz=1.6\mu\text{m}$) the size and velocity PDFs (measured by PDA) do not depend on the x,y position (in the range analysed here). Moreover, the data rate does not depend on the wall distance, and it shows the same time dependence as for the rough surface case (figure 4). The mean diameter d_{10} (evaluated as above the PDA measuring range) time evolution behaves quite similarly to that found for rough surface and figure 5 shows the comparison. It should be pointed out that the difference between curves relative to different wall distances should not be considered significant as the magnitude of diameter rms in each time slot is around

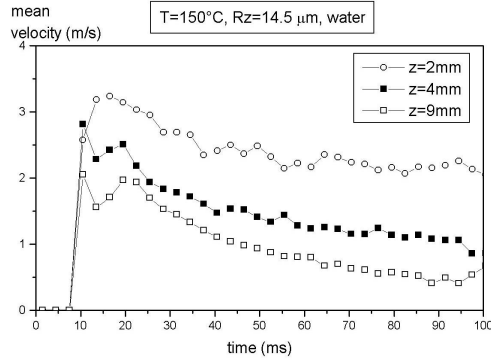


Figure 6. The secondary drop mean velocity evaluated for the size range between 2 and $250\mu\text{m}$ (the PDA measuring range).

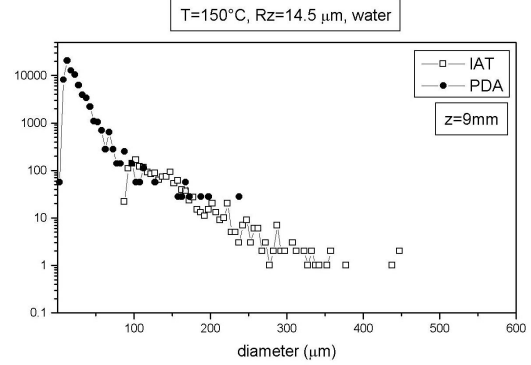


Figure 7. Extended PDF comprising PDA and IAT size measurements for $T=150^\circ\text{C}$ and $Rz=14.5\mu\text{m}$.

100% of mean values. Again there is not any size velocity correlation. The analysis of the images collected allowed to evaluate again the extended PDF. From the quantitative point of view there is not great difference with the results obtained for rough surface, except for the evaluation of the average drop diameter: the d_{10} is comparable to that obtained for the rough surface, whereas the SMD (D_{32}) is smaller (around 25%, see table 2). The analysis on the extended PDF shows that, despite of the difference (although not marked) in morphology, the secondary atomisation characteristics seem not to be strongly influenced by wall roughness in this boiling regime.

2.3. Film boiling regime ($T_w=260^\circ\text{C}$) and rough surface ($Rz=14.5\mu\text{m}$)

PDA measurements in this regime were quite time consuming as after a first burst of secondary drop production (possibly related to a beginning of bubble boiling) the vapour film levitate the liquid from the surface inhibiting bubble formation and the break-up. Also for this regime, the dependence of secondary drop diameter on x,y position (in the analysed region) is neglectful. The measured data rate reported in figure 8 shows the effect above mentioned and observed by the image acquisition: a first burst of droplets (possibly due to the transition from nucleate boiling to film boiling) produced just when drop impacts the hot wall followed by a low amount of drops in the size range measurable by PDA. The IAT analysis shows in fact that the number of drops produced is about one tenth than that observed under the same conditions for bubble boiling regime, whereas the PDFs (and the extended PDFs too) are very similar. It is interesting to compare the results obtained by evaluating the drop size through the extended PDF on both regimes for this wall roughness (see Table 2): the secondary drop diameter is larger (both D_{10} and D_{32}) than that found for film boiling regime, as it was suggested by the qualitative analysis of the images above reported.

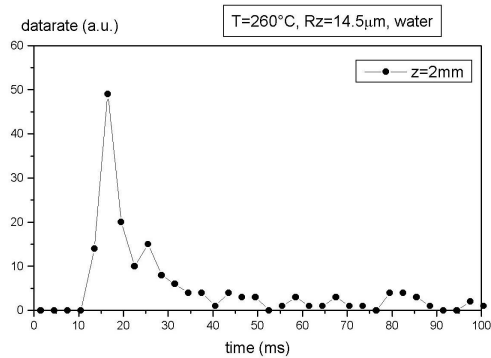


Figure 8. Data rate (PDA) for $T_w=260^\circ\text{C}$ and $Rz=14.5\mu\text{m}$

2.4. Film boiling regime ($T_w=260^\circ\text{C}$) and smooth surface ($Rz=1.6\mu\text{m}$)

Again the data rate evolution is characterised by the burst at the beginning of impact but it reaches a magnitude much lower than the corresponding value for bubble boiling regime. After that, a very small number of droplets reaches the measuring volume and their diameter is much larger than that found in bubble boiling, showing that secondary atomisation is much less efficient under this regime. The evaluation of the extended PDF allowed to measure the average diameters during the first 20 ms after drop impact and table 2 reports the values. It is

diameters	PDA	Extended
D ₁₀ (μm)	22.7	25.3
D ₃₂ (μm)	64.9	105.3

Table1 Comparison between mean diameters evaluated by PDA and by extended PDFs (IAT+PDA) at T_w=150°C and Rz=14.5μm.

diameters	Temperatures	Rz=1.6μm	Rz=14.5μm
D ₁₀ (μm)	150°C	25.58	25.3
	260°C	35.64	46.32
D ₃₂ (μm)	150°C	86.5	105.3
	260°C	221.7	274.1

Table 2 Comparison among the mean diameters (in μm) obtained by extended PDF.

interesting to compare the results obtained with both kind of surfaces: for the film boiling regime the larger roughness surface produces larger droplets (both d_{10} and d_{32}).

Conclusions

At least two different regimes of atomisation as a function of T_w were noticed: a) a bubble boiling regime, for temperature larger than saturation and lower than Leidenfrost, characterised by large production of secondary drops of small size mainly directed along the normal to the wall, b) a film boiling regime, for wall temperature larger than Leidenfrost, characterised by a lower number of secondary drop production of a larger size on the average and a trajectory initially directed tangential to the wall. Many differences in morphology can be observed when the two regimes are compared, among them, the formation of a central jet and the levitation of the liquid lamella with subsequent disruption in larger drops, for film boiling regime, are the most evident. The effect of roughness appears to be more evident for the film boiling regime, both morphologically (disappearing of the central jet, drop ejection characteristics) and quantitatively (increase of the mean drop diameters).

Acknowledgements

The work was partially financed by European project DWDIE (5th framework program) and by the national program PRIN2000.

References

- [1] Marengo M., R. Scardovelli, C. Josserand and S. Zaleski, "Isothermal Drop-Wall Interactions. Introduction to experimental and numerical approaches", in "Navier Stokes Equations: Theory and Numerical Methods", Marcel & Dekker Inc., 2001
- [2] Cossali G.E. Coghe A. and Marengo M.: The impact of a single drop on a wetted solid surface. Experiments in Fluids, vol. 22, pp. 463-472, 1997
- [3] Di Marzo, M., Tartarini, P., Liao, Y., Evans, D., Baum, H. (1993): Evaporative Cooling Due to a Gently Deposited Droplet, Int. J. Heat Mass Transfer, Vol. 36, No. 17, pp. 4133-4139
- [4] Chandra S. e Avedisian C.T. (1991): „On the collision of a droplet with a solid surface“, Proc. Royal Soc. London, 42, pp. 13-41
- [5] Liang Hsing-Sheng, Wen-Jei Yang, Nucleate pool boiling heat transfer in a highly wetting liquid on micro-graphite-fiber composite surfaces, 1998, 41,13, 1993-2001
- [6] Yao S.e Cai K.Y. (1988): „The dynamics and Leidenfrost temperature of drops impacting on a hot surface at small angles“, Exp. Thermal and Fluid Sc., 1, pp. 363-371
- [7] Yao, S., Cai K. Y., 1988, The dynamics and Leidenfrost Temperature of Drops Impacting on a Hot Surface at Small Angles, Exper. Thermal and Fluid Sc., 1, 363-371
- [8] Bernardin J.D., Stebbins C.J., Mudawar I. (1997): „Mapping of impact and heat transfer regimes of water drops impinging on a polished surface“, Int. J. Heat Mass Transfer, Vol. 40, No. 2, pp. 247-267
- [9] Seki, M., Kawamura, H., Sanokawa, K.: Transient Temperature Profile of a Hot Wall Due to an Impinging Liquid Droplet, ASME J. Heat Transfer, Vol. 100 (1978), pp. 167-169
- [10] Di Marzo, M., Tartarini, P., Liao, Y., Evans D., Baum, H. (1991): Dropwise Evaporative Cooling, ASME HTD, Vol. 166, pp.51-58
- [11] Naber J.D. e Farrell P.V. (1993): „Hydrodynamics of droplet impingement on a heated surface“, SAE 930919, pp. 1-16
- [12] Akao F., Araki K., Mori S., Moriyama A. (1980): „Deformation of a liquid droplet impinging onto hot metal surface“, Trans. ISIJ, Vol. 20
- [13] Xiong T.Y. e Yuen M.C. (1991): „Evaporation of a liquid droplet on a hot plate“, Int. J. Heat Mass Transfer, Vol. 34, No. 7, pp. 1881-1894
- [14] Wachters L.H.J. e Westerling N.A.J. (1966): „The heat transfer from a hot wall impinging water drops in the spheroidal state“, Chem. Engineering Sc., 21, pp. 1047-1056
- [15] Araki K. e Moriyama A. (1982): „Deformation behaviour of a liquid droplet impinging on a hot metal surface“, ICLASS '82, pp. 389-396
- [16] Chaves H., Kubitzek A.M., Obermeier F., "Dynamic processes occurring during the spreading of thin liquid films produced by drop impact on hot walls. Heat and Fluid Flows, 20 (1999) 470-476